Biophysical Chemistry 185 (2014) 32–38

Contents lists available at ScienceDirect

Biophysical Chemistry

journal homepage: http://www.elsevier.com/locate/biophyschem

Exploring the energetics of histone H1.1 and H1.4 duplex DNA interactions

V.R. Machha [a], S.B. Jones [a], J.R. Waddle [a], V.H. Le [a], S. Wellman [b], E.A. Lewis [a,*]

[a] Department of Chemistry, Mississippi State University, Box 9573, Mississippi State, MS 39762, USA
[b] Department of Pharmacology and Toxicology, University of Mississippi Medical Center, 2500 North State Street, Jackson, MS 39216-4505, USA

HIGHLIGHTS

- H1.1 and H1.4 bind to DNA oligomers and to CT-DNA with favorable entropy changes.
- The 9 °C increase in T_m for DNA in the H1.4/DNA complex indicates tight binding.
- The H1.4 binding site size was found to be 36.9 bp in titrations of DNA oligomers.
- The H1.1 binding site size was found to be 32 bp in titrations of CT-DNA.
- Loss of water upon H1/DNA complex formation results in large negative ΔC_p values.

GRAPHICAL ABSTRACT

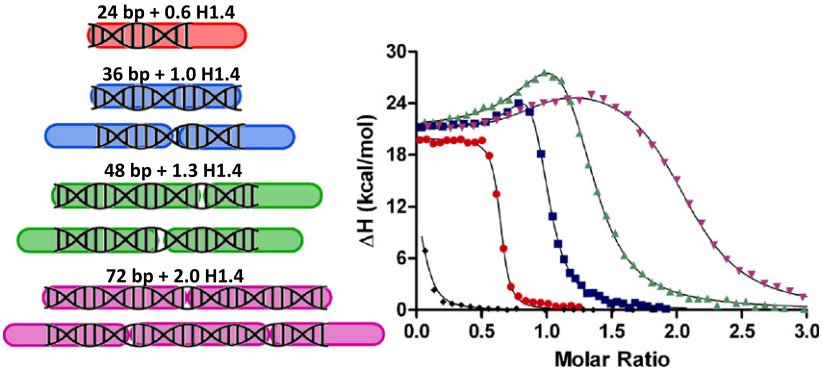

H1.4 Binding Site Size for Complex Formation with DNA Oligomers.

ARTICLE INFO

Article history:
Received 13 September 2013
Received in revised form 28 October 2013
Accepted 18 November 2013
Available online 26 November 2013

Keywords:
Histone
CT-DNA
Chromatin
Chromosome
Nucleosome
ITC

ABSTRACT

H1.1 and H1.4 bind tightly to both short DNA oligomers and to CT-DNA ($K_a \approx 1 \times 10^7$). Binding is accompanied by an unfavorable enthalpy change ($\Delta H \approx +22$ kcal/mol) and a favorable entropy change ($-T\Delta S \approx -30$ kcal/mol). The T_m for the H1.4/CT-DNA complex is increased by 9 °C over the T_m for the free DNA. H1.4 titrations of the DNA oligomers yield stoichiometries (H1/DNA) of 0.64, 0.96, 1.29, and 2.04 for 24, 36, 48, and 72-bp DNA oligomers. The stoichiometries are consistent with a binding site size of 37 ± 1 bp. CT-DNA titration data are consistent with binding site sizes of 32 bp for H1.1 and 36 bp for H1.4. The heat capacity changes, ΔC_p, for formation of the H1.1 and H1.4/CT-DNA complexes are −160 cal mol^{-1} K^{-1} and −192 cal mol^{-1} K^{-1} respectively. The large negative ΔC_p values indicate the loss of water from the protein DNA interface in the complex.

Abbreviations: ITC, Isothermal Titration Calorimetry; CD, Circular Dichroism; CT-DNA, Calf Thymus DNA.

* Corresponding author at: Department of Chemistry, Mississippi State University, 1115 Hand Lab, Box 9573, Mississippi State, MS 39762, USA. Tel.: +1 662 325 3584.
E-mail address: elewis@chemistry.msstate.edu (E.A. Lewis).

0301-4622/$ – see front matter
http://dx.doi.org/10.1016/j.bpc.2013.11.007

1. Introduction

H1 interactions with DNA have attracted significant interest due to the involvement of H1 in chromatin compaction and the fact that H1 is highly modified in cancer cells [1,2]. Histone H1 has also been described as a transcription repressor as it limits the access of transcriptional factor proteins to DNA [2–4]. To date, eleven histone H1 subtypes have been identified in mammals. In both humans and mice, five of the somatic subtypes (H1.1–H1.5) are classified as cell cycle-dependent or replication dependent wherein the expression of these genes is linked to a particular phase of the cell's life cycle. The other somatic subtype, $H1^0$, is classified as replication-independent or replacement subtype and it is expressed throughout the cell's life cycle in order to maintain a replacement pool of H1 linker histone [5]. H1.1 (mouse H1c) and H1.4 (mouse H1e) carry the highest positive charges and exhibit the strongest DNA binding affinities [5,6]. H1.4 is seven amino acids longer (219 vs. 212) than H1.1, with the two sequences exhibiting 89% homology in the N-terminal and globular domains [5]. The larger net positive charge for H1.4 (+59) compared to H1.1 (+55) is due to four additional lysines in the H1.4 sequence. In comparison, $H1^0$ (mouse H1.0) has a net positive charge at neutral pH of +53 and exhibits 61% sequence homology in comparison to the N-terminal and globular domains of H1.1. The C-terminal domains of H1.1, H1.4 and $H1^0$ (wherein most of the charged residues reside) are apparently scrambled and exhibit no sequence homology from a BLAST sequence comparison, http://blast.ncbi.nlm.nih.gov/Blast.cgi [7,8]. Although these three subtypes show similar net charges, high sequence homology in the N-terminal and globular domains, and only subtle changes in overall amino acid composition, it has been reported that the three subtypes exhibit different DNA binding affinities and occupy different DNA binding site sizes [5,6,9]. If there are real differences in the DNA binding affinities or binding site sizes for the H1.1, H1.4 and $H1^0$ proteins, the differences must be attributed to the different sequences and/or charge and charge distribution in the C-terminal domains of these proteins.

It is generally accepted that H1, or linker histone, binds to DNA as it enters and/or exits the nucleosome [10–13]. Two different models for H1 binding place the H1 protein across the nucleosome with H1 interacting with two or three patches of the nucleosomal DNA on the same side of the nucleosome [14] or alternatively locate the H1 so that it binds to a continuous and more linear linker DNA region [15]. The generally accepted biological function for bound H1 is that it prevents nucleosomal DNA from either unraveling from or sliding off the nucleosome histone core complex and that it participates in limited chromatin compaction by tethering adjacent nucleosomes together [10]. Although the structure of the nucleosome (histone core/DNA complex) and the interactions of the core histone proteins with DNA are relatively well established [10,16–19], several questions remain regarding the structural and functional roles of H1 histone in chromatin. Even such basic information as the H1 DNA binding affinity, the H1 DNA binding site size, and the enthalpy and entropy changes for the formation of the H1/DNA complex are largely absent from the current literature. In a previous publication, we reported on the thermodynamics for binding $H1^0$, $H1^0$-C (the C-terminal domain), and $H1^0$-G (the globular domain) to highly polymerized calf thymus DNA [9]. Perhaps the most surprising result of the previous study was the fact that the ΔH values for formation of the $H1^0$/DNA and $H1^0$-C/DNA complexes were highly endothermic ($\Delta H \approx +22$ kcal/mol). In contrast, a recent publication by Caterino et al. reported that the enthalpy change for binding the H1 carboxy terminal domain to linker DNA is −12 kcal/mol. The Caterino enthalpy data were obtained indirectly from a van't Hoff analysis of K_a vs. T experiments with the K_a values determined in gel (GMSA) experiments [20].

In the present study we have used isothermal titration calorimetry (ITC), differential scanning calorimetry (DSC), and CD spectropolarimetry to determine the thermodynamic signatures and structural changes that accompany H1.1 and H1.4 binding to short DNA oligomers and/or H1.1 and H1.4 binding to highly polymerized calf-thymus DNA. The results from these studies on H1.1 and H1.4 were compared to published results of similar studies don on $H1^0$ [9]. In our ITC studies, we found that the H1.1 and H1.4 bind to CT-DNA with approximately the same affinity observed previously for $H1^0$ ($K_a \approx 1 \times 10^7$). We also observed large endothermic enthalpy changes for the formation of the H1.1/DNA and H1.4/DNA complexes ($\Delta H \approx +22$ kcal/(mol H1.1 or H1.4)) which were again similar to the ΔH value observed for the formation of the $H1^0$/CT-DNA complex [9]. The binding site sizes for H1.1 and H1.4 were determined to be 32 bp and 36 bp, respectively. The change in the binding site size between H1.1 and H1.4 seems anomalously large since the two proteins are different by only 3% in molecular weight. Interestingly, the binding site size for the smallest H1 subtype, $H1^0$, was also determined to be 36 DNA bp [9]. Titrations of short double stranded DNA oligomers (having from 12 to 72 bp) yield H1.4 binding stoichiometries (H1.4/DNA bp) that are in excellent agreement with the H1.4 binding site size determined in H1.4 CT-DNA titrations DSC determined T_m values indicate that the melting temperature of the CT-DNA in the H1.4/CT-DNA complex is increased by 9 °C, a result that is in agreement with the high H1.4 DNA binding affinity. CD experiments indicate that DNA is restructured upon complex formation with either the H1.1 or H1.4, again a result that is similar to the changes in CD spectrum that accompany formation of the $H1^0$/CT-DNA complex. In contrast, the H1 protein structure (H1.1, H1.4, or $H1^0$) is largely unchanged upon formation of the H1/DNA complexes. ΔC_p values determined for the formation of the H1.1 and H1.4 CT-DNA complexes are large and negative (e.g. −160 or −192 cal mol^{-1} K^{-1}). Large negative ΔC_p values had also been observed previously for the formation of the $H1^0$/CT-DNA complex. These large negative ΔC_p values are indicative of the loss of water from either the DNA (or the protein) as the H1/DNA complexes are formed. All of these results are placed in the context of the current histone literature and are discussed more fully in the later sections of this work.

2. Materials and methods

2.1. Proteins and DNA samples

The two histone H1 variants, H1.1 and H1.4, were expressed using a bacterial strain of *E. coli* (*Rosetta (De3) pLysS*) infected with a pET-11d (Novagen) expression vector which contained the DNA sequence for either the mouse H1.1 protein or the mouse H1.4 protein. The constructions of the expression strains, induction, extraction, and purification have been described [21,22]. The pure protein fractions were concentrated using a Savant SPD 111 V speed vac system for 4 hrs at 35 °C to remove the HPLC solvent (5% acetonitrile/95% water). Calf thymus DNA type I was purchased from Sigma (St. Louis, USA) and used without further purification. Short double stranded DNAs designed for the H1.4 ITC binding studies were purchased from Midland Certified reagent Company (Midland TX, USA) (The sequences for the short duplex DNAs are given in Table 1). The protein and DNA stock solutions were prepared by dissolution of the concentrated and/or dried purified protein or DNA samples in the standard BPES buffer (30 mM K_2HPO_4/KH_2PO_4 (pH = 7.0), 1 mM EDTA, and 100 mM KCl). The protein and DNA stock solutions were exhaustively dialyzed against the sample buffer (24 h) at 4 °C, using a 1000 Mw cutoff dialysis membrane (Thermo Scientific, USA). Calf thymus DNA concentrations in base pairs (bp) were determined using measured absorbance at 260 nm and a molar extinction coefficient of $\varepsilon_{260} = 1.31 \times 10^4$ bp M^{-1} cm^{-1} [23]. The approximate average molecular weight of the CT-DNA was 8.4×10^3 kDa (Sigma, St. Louis, USA). Short DNA oligomer concentrations were determined using absorbance values at 260 nm and molar extinction coefficients (ε_{260}) of 1.912×10^5, 3.806×10^5, 5.710×10^5, 7.634×10^5, and 11.421×10^5 M^{-1} cm^{-1} for 12-mer, 24-mer, 36-mer, 48-mer, and 72-mer respectively. H1.1 and H1.4 concentrations were determined by UV absorbance measurements at 205 nm and using extinction coefficients of 6.37×10^5 M^{-1} cm^{-1},

Table 1
Short synthetic duplex DNAs designed for H1.4 ITC binding studies.

12-mer (T_m = 36.0 °C)
5′-ATCAAGCTACGC-3′
3′-TAGTTCGATGCG-5′
24-mer (T_m = 57.4 °C)
5′-ATCAAGCTACGCCTGAAGAGTCTG-3′
3′-TAGTTCGATGCGGACTTCTCAGAC-5′
36-mer (T_m = 67.9 °C)
5′-ATCAAGCTACGCCTGAAGAGTCTGGTGAGCAAGGGT-3′
3′-TAGTTCGATGCGGACTTCTCAGACCACTCGTTCCCA-5′
48-mer (T_m = 72.2 °C)
5′-ATCAAGCTACGCCTGAAGAGTCTGGTGAGCAAGGGTACTCTGGTGTAG-3′
3′-TAGTTCGATGCGGACTTCTCAGACCACTCGTTCCCATGAGACCACATC-5′
72-mer (T_m = 76.6 °C)
5′-ATCAAGCTACGCCTGAAGAGTCTGGTGAGCAAGGGTACTCTGGTGTAGACCAAGTGCA CTGGTCCTTCAATC-3′
3′-TAGTTCGATGCGGACTTCTCAGACCACTCGTTCCCATGAGACCACATCTGGTTCACGT GACCAGGAAGTTAG-5′

and 6.11×10^5 M^{-1} cm^{-1} for H1.1 and H1.4 respectively [24]. The approximate molecular weights for the H1.1 and H1.4 were estimated from their sequences using the ExPASy ProtParam tool (http://web.expasy.org/protparam): Mw (H1.1) ≈ 21.3 kDa, Mw (H1.4) ≈ 21.9 kDa.

2.2. Isothermal titration calorimetry

Isothermal titration calorimetry (ITC) experiments were performed using a Microcal VP-ITC (Northampton, MA, USA). All titrations were performed by overfilling the ITC cell with approximately 1.5 mL of dilute DNA solution (nominally 540 μM in bp). During a typical ITC titration, approximately 250 μL of the H1.1 or H1.4 protein solution was added to the DNA solution in the micro-calorimeter cell in 25 to 50 increments delivered at 600 second intervals. All of our ITC experiments were performed in triplicate and at three different temperatures, 15 °C, 25 °C, and 35 °C. The integrated heat/injection data were fit for an appropriate thermodynamic model using CHASM data analysis software developed in our laboratory [25]. The non-linear regression fitting process yields best fit parameters for K (or ΔG), ΔH, ΔS, and n for each independent interaction.

2.3. Differential scanning calorimetry

Differential scanning calorimetry (DSC) experiments were performed using a Microcal VP-DSC (Northampton, MA, USA). The melting temperatures, T_m, were determined for CT-DNA and H1.4/CT-DNA in separate DSC experiments. The nominal DNA concentration for these experiments was 2.16 mM (in bp), and the complex was prepared by the addition H1.4 protein to the 2.16 mM DNA solution to yield a final H1.4 concentration of 0.012 mM (assuming an approximate DNA binding site size of 36 bp/H1.4, this solution had a nominal composition of 0.2 equivalents of H1.4 protein per equivalent of DNA sites). The temperature scan range in these experiments was 10 to 110 °C with a scan rate of 90 °C/hr. The CT-DNA denaturation over this temperature range was irreversible; therefore only one heating scan was performed in each experiment. The irreversibility in these experiments was due to aggregation and precipitation of the high molecular weight DNA. Because the aggregation and precipitation is slow and displace in time from the helix to coil transition, the determination of the thermodynamic parameters for DNA denaturation is valid. the DSC data from the first scan were therefore fit for ΔH_{cal}, ΔH_{VH}, and the melting temperature (T_m) using the "two-state" model in Origin 7.1 software (Microcal, Northampton, MA).

2.4. Circular dichroism

CD experiments were performed using an Olis DSM 20 spectropolarimeter (Bogart, GA). CT-DNA and protein solutions were prepared with a nominal absorbance of 0.5 AU in a nominal 50 mM KBPES buffer (pH = 7.0, 10 mM KCl, 30 mM Phosphate, 0.1 mM EDTA). In these experiments, the nominal concentration of the protein was 1.5 μM, and the concentration of the CT-DNA was 3.0 μM in H1 binding sites. The 0.5:1 mole ratio for protein to DNA binding sites was chosen to avoid the complications that appear near the endpoint in the ITC titrations.

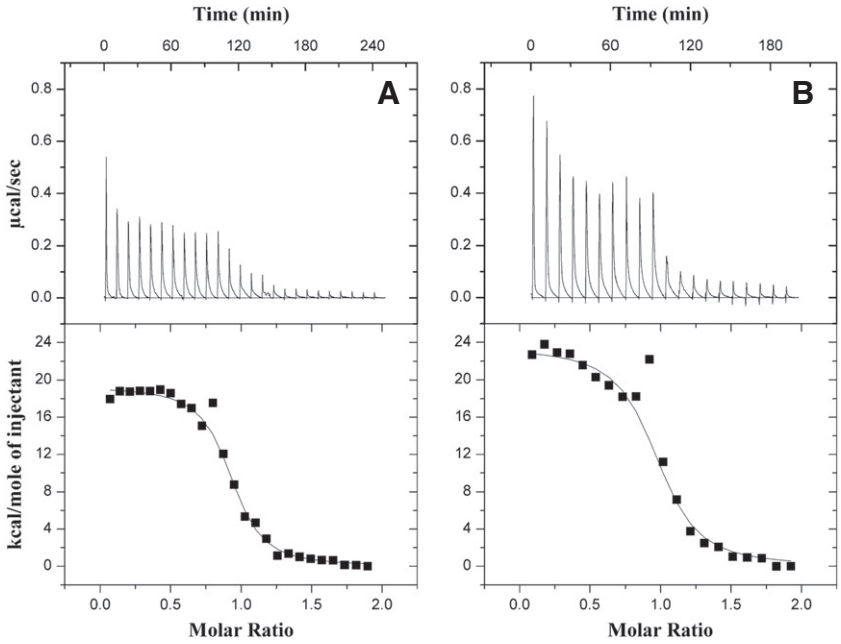

Fig. 1. Panel **A** shows a typical ITC titration for the addition of H1.1 to highly polymerized CT-DNA. The upper half of Panel **A** shows the baseline-corrected raw ITC signal for 25 injections of a dilute H1.1 protein solution (10 μL of 135 μM H1.1) into the ITC cell filled with a dilute solution of CT-DNA (13 μM in H1.1 binding sites). The lower half of Panel **A** shows the apparent ΔH for each injection (■) along with the best-fit non-linear regression line (–) for a one site binding model. Panel **B** shows a typical ITC titration for the addition of H1.4 to highly polymerized CT-DNA. The upper half of Panel **B** shows the baseline-corrected raw ITC signal for 20 injections of a dilute H1.4 protein solution (14 μL of 140 μM H1.4) into the ITC cell filled with a dilute solution of CT-DNA (15 μM in H1.4 binding sites). The lower half of Panel **B** shows the ΔH for each injection (■) along with the best-fit non-linear regression line (–) for a one site binding model.

We used diluted solutions of both protein and DNA, and used excess moles of DNA to prepare complex samples for the CD experiments to minimize complex aggregation. CD spectra were collected over a wavelength range from 200 to 300 nm (with measurements every 0.5 nm) in a 1 cm path length cuvette at room temperature. The spectra represent the average of three scans which were processed using PRISM software (graph-Pad Prism Software, San Diego, CA).

3. Results

3.1. ITC

Fig. 1 shows typical ITC data for titrations of the H1.1 and H1.4 proteins into highly polymerized CT-DNA at 25 °C. The ITC thermograms were fit using non-linear regression techniques to a multiple independent site model (one site model) and the average best-fit parameters are listed in Table 2. We also attempted to fit these titration data to a nearest neighbor exclusion model [26], however, the multiple sites do not appear to be interacting and do not exhibit either positive or negative cooperativity. This was determined from the independence of ΔH on degree of saturation, ($\Delta h \approx 0.0$). ITC data indicate that although H1.1 or H1.4 have a high binding affinity ($K \approx 10^7\ M^{-1}$) for CT-DNA, the enthalpy change is very unfavorable ($\Delta H \approx +22$ kcal/(mol H1.1 or H1.4)) and complex formation is driven by a large favorable entropy change ($-T\Delta S \approx -30$ kcal/mol). The anomalously large endothermic heat values that are observed as one or two points that are significantly above the best fit line and just prior to the end point in both ITC titrations (Fig. 1A, B) are attributed to overcoming a steric interaction in which a bound protein is partially occupying two adjacent sites and this protein must be relocated in order to fully populate all of the potential protein binding sites on the DNA. The additional endothermic heat observed near saturation represents the energy cost of relocating the one or more already bound proteins that are unevenly distributed along the linear lattice of the DNA. In effect as H1.1 (or) H1.4 binds non-specifically (electrostatically) to a long DNA molecule, the placement of the proteins is random and can result in multiple partial binding sites that are vacant. The binding-site size, or the number of base pairs occupied per bound H1.1 or H1.4 protein, was calculated from the ratio of added protein at the titration endpoint to the total number of DNA base pairs in the calorimeter. The saturation stoichiometry indicated that one mole of H1.1 binds to 32 bp and one mole of H1.4 binds to 36 bp. To further probe the accuracy of binding site size in more detail, we titrated H1.4 into short random sequence ds-DNA solutions (12 bp, 24 bp, 36 bp, 48 bp, and 72 bp). In Fig. 2, we have plotted the apparent ΔH values for each injection along with the best-fit non-linear regression line against to the molar ratio (H1/DNA oligomer) for each titration. Table 3 lists the stoichiometries and the enthalpy values for the titrations of H1.4 into short ds-DNA sequences. These results are discussed in more detail in the discussion section of the paper. We also performed a temperature dependent study in which the experiments shown in Fig. 1 were repeated at 15 °C and 35 °C. In Fig. 3, we have plotted the values for ΔH binding H1.1 and H1.4 to CT-DNA as a function of temperature. Both H1.1 and H1.4 showed a linear decrease in enthalpy change with increasing temperature. The slope of the linear least squares fits to all data for both H1.1 and H1.4 yielded large negative ΔC_p values of -160 and -192 cal mol^{-1} K^{-1} respectively.

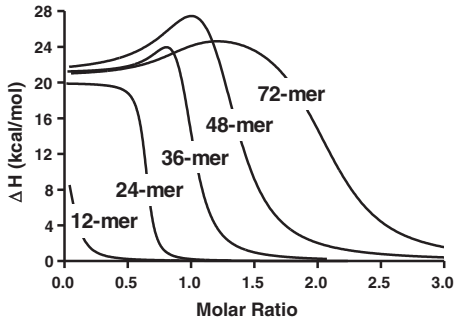

Fig. 2. ITC titration curves for the addition of H1.4 (140 μM) into dilute solutions (10 μM) of short DNA duplex oligomers. The data for the 12-bp and 24-bp oligomers were fit to a one site thermodynamic model whereas the 36-bp, 48-bp, and 72-bp oligomer data were fit to a two site thermodynamic model. The best fit parameters (n_1, ΔH_1, n_2, and ΔH_2) are listed in Table 3.

3.2. CD

CD experiments were used to detect gross structural changes in the DNA and the histone variants upon formation of the histone/DNA complex. Fig. 4A shows representative CD spectra for the H1.1 histone protein, CT-DNA and the spectrum for the 0.5:1 complex of H1.1/CT-DNA. Fig. 4B shows representative CD spectra for the H1.4 histone protein, CT-DNA and the spectrum for the 0.5:1 complex of H1.4/CT-DNA. The CT-DNA spectrum shows a positive molar ellipticity at 280 nm and a negative molar ellipticity at 245 nm that is consistent with CD spectra previously reported for CT-DNA [27,28]. The H1 protein spectrum exhibits a negative molar ellipticity at 208 and 222 nm indicative of a significant amount of α-helix and β-turn present in the structure of the histone protein [29]. The CD spectra obtained for the H1.1 and H1.4 closely resemble the CD spectrum reported for H1 by Barbero et al. [30]. Both H1.1 and H1.4 also exhibit CD spectra that are similar to the spectrum reported for H5, which includes structural contributions from the globular domain [31]. The complex spectra for H1.1/CT-DNA and H1.4/CT-DNA (Fig. 4A and B) exhibit some changes to the DNA structure while the structures of the H1.1 and H1.4 proteins appear to be largely unchanged. Specifically the DNA peak at approximately 280 nm is completely lost. The DNA negative ellipticity at approximately 245 nm is canceled out by the protein positive ellipticity in the same

Table 2
ITC derived thermodynamic parameters for H1.1 and H1.4 histone protein binding to CT-DNA in 100 mM [K^+] BPES pH 7.0 at 25 °C.

	K_a (M^{-1}) $\times 10^{-6}$	ΔG (kcal/mol)	ΔH (kcal/mol)	$-T\Delta S$ (kcal/mol)	Binding site size (bp)
H1.1	6.3 ± 0.1	−9.3	18.2 ± 0.8	−27.5	32
H1.4	3.2 ± 0.3	−8.9	22.5 ± 0.5	−31.4	36

All ITC experiments were performed in triplicate in 100 mM [K^+] BPES buffer at pH 7.0 and 25 °C. The integrated heat/injection data were fit for to a one site thermodynamic model using CHASM data analysis software developed in our laboratory. Errors listed are the standard deviations for the best fit parameters K and ΔH determined in triplicate experiments. Effective binding site size in base pairs was calculated from the titration endpoint, the DNA concentration in base pairs and the assumption that saturation stoichiometry is 1:1 (H1:DNA sites).

Table 3
ITC derived thermodynamic parameters for H1.4 histone protein binding to short ds-DNA oligomers in 100 mM [K^+] BPES pH 7.0 at 25 °C.

Oligo	n_{total}	Binding site size (bp)	n_1	ΔH_1 (kcal/mol)	n_2	ΔH_2 (kcal/mol)
24-mer	0.64	37.5	0.64 ± 0.00	20.0 ± 0.2	–	–
36-mer	0.96	37.5	0.84 ± 0.06	21.4 ± 0.3	0.12 ± 0.08	55 ± 28
48-mer	1.29	37.2	0.94 ± 0.10	21.1 ± 0.7	0.35 ± 0.10	50 ± 15
72-mer	2.04	35.3	0.87 ± 0.08	20.7 ± 0.6	1.18 ± 0.09	27.8 ± 1.2

All ITC experiments were performed in triplicate in 100 mM [K^+] BPES buffer at pH 7.0 and 25 °C. The integrated heat/injection data were fit for to a fractional site thermodynamic model in which the first fractional reaction is for the simple binding of the protein to the DNA and the second fractional interaction includes both binding and the energetic for rearrangement of the bound protein to maximize the available binding site area. The total n ($n_1 + n_2$) is determined from the titration endpoint. The non-linear regression fits were done using CHASM data analysis software developed in our laboratory. Errors listed are the standard deviations for the best fit parameters n_1, n_2, ΔH_1, and ΔH_2 determined in triplicate experiments. Effective binding site sizes in base pairs were calculated from the titration endpoint, the DNA concentration in base pairs and the assumption that saturation stoichiometry is 1:1 (H1:DNA sites).

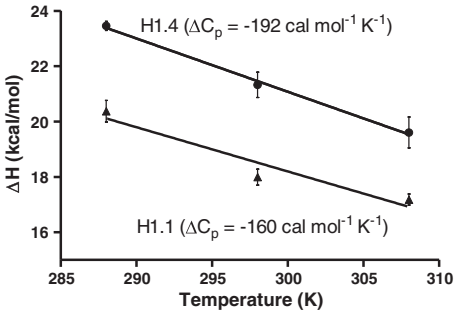

Fig. 3. A plot of the ITC derived ΔH values for the formation of the H1.1 and H1.4/CT-DNA complexes vs. temperature. Data are shown for three temperatures: 15, 25, and 35 °C. The slopes of the two lines yield estimates for the ΔC_p values that accompany the formation of the H1.1 and H1.4/CT-DNA complexes.

wavelength range. In contrast, the characteristic CD spectrum for the protein (H1.1 and H1.4) is almost unchanged especially over the 200 to 230 nm range in the complex. Clearly this indicates that the H1 α-helix and β-turn structure persists in the H1/CT-DNA complex.

3.3. DSC

Differential scanning calorimetry was used to determine the stability of the histone/DNA complex versus the stability of the uncomplexed CT-DNA. The DSC melting profiles for the thermal denaturation of the CT-DNA as well as the H1.4/CT-DNA complex are shown in Fig. 5. The CT-DNA thermogram is comprised of a single symmetric peak that has been fit for a "two state" transition (see Fig. 5A). The CT-DNA melting temperature determined here (84.0 °C) is in reasonable agreement with previously reported T_m values for CT-DNA [32,33]. The DSC data shown in Fig. 5B show melting transitions for CT-DNA and the H1.4/CT-DNA complex after the addition of approximately 0.2 equivalents of protein per equivalent of protein binding sites. This thermogram has been fit for two independent overlapping "two-state" processes with T_m values of 83.7 °C and 92.8 °C. The lower melting peak is attributed to denaturation of the free CT-DNA in solution while the higher melting peak is attributed to denaturation of the protein stabilized DNA in the H1.4/CT-DNA complex. The lower temperature peak corresponds to the melting of approximately 80% of the total DNA while the higher temperature peak corresponds to melting approximately 20% of the total DNA. These values are consistent with the approximate composition of the sample.

4. Discussion

The main purpose of this study was to determine the thermodynamic parameters for the binding of H1.1 and H1.4 variants to variable length ds-DNA such as short sequence DNA oligomers and to highly polymerized calf-thymus DNA, and to compare the thermodynamics for these two H1 variants to $H1^0$ [9]. ITC studies demonstrated that the binding of H1.1 and H1.4 to CT-DNA was accompanied by a large unfavorable enthalpy change which is compensated by an even larger favorable entropy change. The large positive entropy change ($-T\Delta S \approx -30$ kcal/(mol H1)) and positive enthalpy change ($\Delta H \approx +22$ kcal/(mol H1)) terms are consistent with the release of ordered water molecules from the backbone and grooves of the DNA upon H1 complex formation. We have used a multiple equivalent sites (one site) model to fit the ITC titration data. One anomaly that is observed in the thermograms for the titration of CT-DNA with $H1^0$, H1.1 and H1.4 is one or more larger endothermic peak in the thermogram that are seen just before the DNA is saturated with protein. We attribute the anomalously large endothermic point(s) observed immediately before the end point in the $H1^0$, H1.1, and H1.4 DNA titrations to the rearrangement of non-specifically bound H1 along the length of the

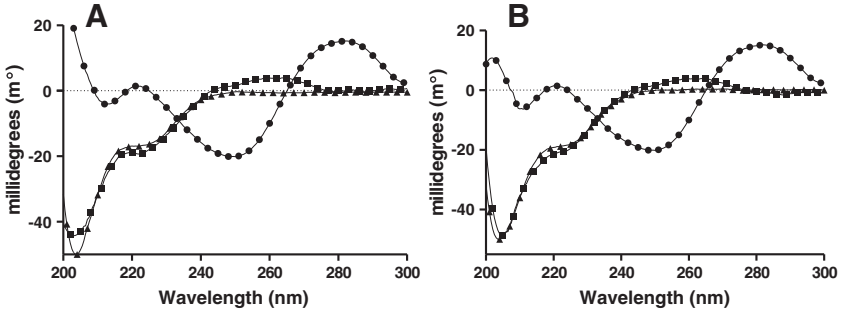

Fig. 4. Panel **A** shows the CD spectra for the H1.1 protein (-▲-), CT-DNA (-●-), and the 0.5:1 H1.1/CT-DNA complex (-■-). Panel **B** shows the CD spectrum for the H1.4 protein (-▲-) along with the spectra for CT-DNA (-●-), and the 0.5:1 H1.4/CT-DNA complex (-■-).

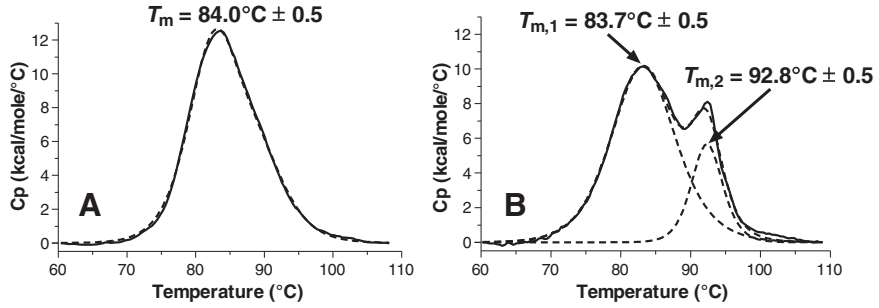

Fig. 5. Panel **A** shows the DSC thermogram for the thermal denaturation of CT DNA. The raw excess heat capacity (solid line) has been deconvoluted into a single "non two-state" process (—). Panel **B** shows the DSC thermogram for the thermal denaturation of Histone H1.4 and its complex with CT-DNA in 100 mM KCl BPES. The excess heat capacity for the H1.4/CT-DNA complex has been deconvoluted into two independent overlapping "two-state" processes (—). The lower melting profile is attributed to "free" CT-DNA while the higher melting transition is for the melting of the H1.4/CT-DNA stabilized complex.

DNA. Binding of the H1 protein to ds-DNA is non-specific (i.e. the protein does not target a specific DNA sequence or region) [34–36]. As the protein concentration approaches DNA saturation, randomly bound protein may be "rearranged" along the DNA in order to minimize the number of partially obscured H1 binding sites and thereby maximize the number of available protein binding sites. The endpoints in the ITC thermograms were used along with the DNA concentration in base pairs to estimate the number of base pairs covered by the binding of 1 mole of H1 protein. This analysis yielded estimates of 32 bp and 36 bp for the H1.1 and H1.4 binding site sizes respectively. Since some H1 binding sites (or partial binding sites) may be unoccupied at the ITC endpoint (saturation point), these values represent an upper limit on the number of DNA base pairs that may correspond to the actual binding site size.

To further probe the issue of binding site size for the interactions of H1 proteins with duplex DNA, H1.4 was titrated into solutions containing short ds-DNA oligomers having 12, 24, 36, 48 or 72 bp. These data which are shown in Fig. 2 have been fit to a thermodynamic model in which the saturated complex is the result of at least two competing processes. Fitting the ITC data to a fractional sites model yields two values for each of the thermodynamic parameters (K, ΔH, and n), with the first set of parameters applicable to the interaction of the protein and DNA at low site occupancy and the second set of parameters applicable for the interaction of the protein and DNA at high site occupancy or near saturation. The thermodynamic parameters listed in Table 3 assume a one to one correspondence between the number of bound protein molecules and the number of sites provided on one mole of the ds-DNA oligomer. In effect the shorter DNA oligomers (12 and 24-mers) were only long enough to bind a short part of a single protein molecule while the longer DNA oligomers (48 and 72-mers) were long enough to bind more than one complete protein molecule. The end points for the ITC titration curves shown in Fig. 2 can thus be used to directly estimate the binding site size in DNA base pairs for binding one mole of H1.4. The CT-DNA titration data yielded an approximate binding site size of 36 bp for H1.4 while the short DNA titrations yielded an average value of 36.9 bp. Obviously the agreement in binding site size as determined in titration experiments done on poly-disperse, highly polymerized CT-DNA and the experiments employing 5 different mono-disperse low molecular weight DNAs is very good.

The anomaly in the enthalpy curve only begins to appear when more than one mol of protein (e.g. 1.2 to 2.0 mols of protein) is bound to a single DNA oligomer. In effect, it is only when the DNA is fully covered with protein (or when available sites are fully populated) with bound protein that the excess endotherm for protein rearrangement along the DNA is observed. In the high molecular weight CT-DNA the anomaly in apparent ΔH is limited to one or two points in the thermogram whereas in the short oligomer titrations the effect is more pronounced since the binding of a second protein (even if it is only partially overlapping available base pairs) occurs almost throughout the titration.

In our previous study of $H1^0$ binding to CT-DNA we had determined that the release of bound counterions (e.g. Na^+, or K^+) upon $H1^0$ complex formation was limited, ($\delta n_K^+ \approx 1$) [9]. Since the net charges, protein sizes, and amino acid composition of all three proteins are very similar, we have made the assumption that the counterions released upon binding H1.1 or H1.4 to CT-DNA would be similar to what we had previously seen for $H1^0$. The slopes from the temperature dependent ITC data shown in Fig. 3 for binding H1.1 and H1.4 to CT-DNA, i.e. plots of ΔH vs. temperature, are indicative of large negative heat capacity changes, ΔC_p, for the formation of the H1.1 and H1.4, CT-DNA complexes. We had also observed a large negative heat capacity change for formation of the $H1^0$/CT-DNA complex (data not shown). Our CD results appear to rule out any significant macromolecule structural change contributions to either the large positive ΔS values or to the large negative ΔC_p values. Since macromolecular structural changes and the release of bound counterions have been ruled out, these large negative ΔC_p values must be due to the release of a large number of water molecules upon formation of the $H1^0$, H1.1, and H1.4, complexes with CT-DNA.

CD results indicate that the two peaks attributed to CT-DNA, i.e. 245 and 280 nm, were both attenuated upon formation of the H1.1/CT-DNA (or H1.4/CT-DNA) complex. This is consistent with a conformational change in DNA that is induced by $H1^0$, H1.1 or H1.4 binding. This result is consistent with several previous studies which have suggested that binding the H1 C-terminal domain to DNA causes bending of chromatosomal DNA to facilitate a stem-like structure [37,38]. The structural stabilization of the H1.4 protein/DNA complex was further characterized using DSC. A single ("two-state") transition occurring at 84 °C was observed for the denaturation of the CT-DNA in the absence of the protein. After the addition of 0.2 equivalents of H1.4 protein per equivalent of DNA protein binding site, a second melting profile appeared with a T_m value of approximately 93 °C. This higher melting transition is for the melting of the H1.4 protein stabilized DNA in the complex. The peak area of the higher melting transition is approximately 1/5 of the area for CT-DNA alone which is consistent with 20% of the binding sites being occupied in the 20% saturated H1.4/CT-DNA complex. The 9 °C shift in the melting temperature of the protein bound DNA is consistent with a binding constant of 10^7 which is in excellent agreement with K_a value determined for H1.4 binding in the ITC experiments.

There are two distinctly different models in the current literature which describe the function of H1 linker in compacting and stabilizing the nucleosome [14,15]. In the dyad axis model, the linker H1 globular domain is bound to two widely separated DNA domains or patches on one side of the nucleosome. The bound H1 globular domain is approximately centered on the nucleosome's dyad axis [14]. In this model, the two DNA H1 binding sequences are separated along the length of the nucleosomal DNA from a minimum of approximately 82 bp to a maximum of approximately 168 bp. In the off-dyad axis model, the linker H1 globular domain binds to only one patch of DNA located at either the point where DNA is beginning to wrap on the nucleosome or the point where DNA is leaving the nucleosome [15]. In this model only one DNA domain is interacting with globular domain of bound H1 and the H1 binding site consists of a continuous stretch of DNA. In both models, the H1 N-terminal tail binds to a short continuous fragment of nucleosomal DNA while the H1 C-terminal tail binds to a longer continuous fragment of linker DNA that bridges between two adjacent nucleosomes. Although both the nucleosomal DNA and linker DNA are probably bent, these stretches of continuous DNA that interact with the H1 tails should be reasonably well modeled by the DNA substrates used in this study. Although not bent, DNA oligomers as short as 36 bp would correspond to one third of one DNA turn around the nucleosome. While actual nucleosomes may have provided a better protein binding substrate (or template) for exploring H1 binding to bent or curved DNA, the binding of $H1^0$, H1.1, and H1.4 to linear DNA (either short DNA oligomers or CT-DNA) seems to provide a consistent picture with respect to binding affinity, the enthalpy and entropy changes for H1 binding, and the number of DNA bp covered by bound H1 in formation of these complexes. Our most puzzling result is that the enthalpy change results determined by Caterino et al. are completely opposite in sign, i.e. exothermic rather than endothermic, from the ΔH values determined here [20]. We can only suggest that the gel mobility shift assays done as a function of temperature by Caterino were flawed in some way. Perhaps changes in gel porosity with temperature lead to inaccurate K_d's and to their conclusion that the binding of Histone H1 to nucleosomal DNA is exothermic. The large differences in the reported ΔH values, for formation of the H1 DNA complexes, ranging from −12 Kcal/mol [20] to +22 kcal/mol, would serve to demonstrate the need for studies like the one reported here.

In conclusion, this study clearly shows that H1.1 and H1.4 behave very similarly to $H1^0$ in forming high affinity complexes with highly polymerized calf-thymus DNA. In addition, the binding of H1.4 to short DNA oligomers confirms both the limiting binding site size and the thermodynamics for the H1 DNA interactions. The formation of

the $H1^0$, H1.1, and H1.4 DNA complexes is driven primarily by large favorable entropy changes. It would appear that these large positive entropy changes result primarily from the expulsion of bound water molecules from the protein/DNA binding interface.

Appendix A. Supplementary data

Supplementary data to this article can be found online at http://dx.doi.org/10.1016/j.bpc.2013.11.007.

References

[1] S. De, D.T. Brown, Z.H. Lu, G.H. Leno, S.E. Wellman, D.B. Sittman, Histone H1 variants differentially inhibit DNA replication through an affinity for chromatin mediated by their carboxyl-terminal domains, Gene 292 (2002) 173–181.
[2] P.S. Espino, B. Drobic, K.L. Dunn, J.R. Davie, Histone modifications as a platform for cancer therapy, J. Cell. Biochem. 94 (2005) 1088–1102.
[3] Y. Fan, T. Nikitina, J. Zhao, T.J. Fleury, R. Bhattacharyya, E.E. Bouhassira, A. Stein, C.L. Woodcock, A.I. Skoultchi, Histone H1 depletion in mammals alters global chromatin structure but causes specific changes in gene regulation, Cell 123 (2005) 1199–1212.
[4] G.E. Croston, L.A. Kerrigan, L.M. Lira, D.R. Marshak, J.T. Kadonaga, Sequence-specific antirepression of histone H1-mediated inhibition of basal RNA polymerase II transcription, Science 251 (1991) 643–649.
[5] N. Happel, D. Doenecke, Histone H1 and its isoforms: contribution to chromatin structure and function, Gene 431 (2009) 1–12.
[6] M. Orrego, I. Ponte, A. Roque, N. Buschati, X. Mora, P. Suau, Differential affinity of mammalian histone H1 somatic subtypes for DNA and chromatin, BMC Biol. 5 (2007) 22.
[7] S.F. Altschul, T.L. Madden, A.A. Schaffer, J. Zhang, Z. Zhang, W. Miller, D.J. Lipman, Gapped BLAST and PSI-BLAST: a new generation of protein database search programs, Nucleic Acids Res. 25 (1997) 3389–3402.
[8] S.F. Altschul, J.C. Wootton, E.M. Gertz, R. Agarwala, A. Morgulis, A.A. Schaffer, Y.K. Yu, Protein database searches using compositionally adjusted substitution matrices, FEBS J. 272 (2005) 5101–5109.
[9] V. Machha, J.R. Waddle, A.L. Turner, S. Wellman, V.H. Le, E.A. Lewis, Calorimetric studies of the interactions of linker histone H10 and its carboxyl (H10-C) and globular (H10-G) domains with calf-thymus DNA, Biophys. Chem. 184 (2013) 22–28.
[10] A. Ramaswamy, I. Bahar, I. Ioshikhes, Structural dynamics of nucleosome core particle: comparison with nucleosomes containing histone variants, Proteins 58 (2005) 683–696.
[11] A.J. Andrews, K. Luger, Nucleosome structure(s) and stability: variations on a theme, Annu. Rev. Biophys. 40 (2011) 99–117.
[12] C.L. Woodcock, R.P. Ghosh, Chromatin higher-order structure and dynamics, Cold Spring Harb Perspect Biol 2 (2010) a000596.
[13] C.L. Woodcock, Chromatin architecture, Curr. Opin. Struct. Biol. 16 (2006) 213–220.
[14] Y.B. Zhou, S.E. Gerchman, V. Ramakrishnan, A. Travers, S. Muyldermans, Position and orientation of the globular domain of linker histone H5 on the nucleosome, Nature 395 (1998) 402–405.
[15] D. Pruss, A.P. Wolffe, Histone–DNA contacts in a nucleosome core containing a *Xenopus* 5S rRNA gene, Biochemistry 32 (1993) 6810–6814.
[16] K. Luger, A.W. Mader, R.K. Richmond, D.F. Sargent, T.J. Richmond, Crystal structure of the nucleosome core particle at 2.8 A resolution, Nature 389 (1997) 251–260.
[17] R.K. Suto, M.J. Clarkson, D.J. Tremethick, K. Luger, Crystal structure of a nucleosome core particle containing the variant histone H2A.Z, Nat. Struct. Biol. 7 (2000) 1121–1124.
[18] C. Zheng, J.J. Hayes, Intra- and inter-nucleosomal protein–DNA interactions of the core histone tail domains in a model system, J. Biol. Chem. 278 (2003) 24217–24224.
[19] L. Marino-Ramirez, M.G. Kann, B.A. Shoemaker, D. Landsman, Histone structure and nucleosome stability, Expert Rev. Proteomics 2 (2005) 719–729.
[20] T.L. Caterino, H. Fang, J.J. Hayes, Nucleosome linker DNA contacts and induces specific folding of the intrinsically disordered H1 carboxyl-terminal domain, Mol. Cell. Biol. 31 (2011) 2341–2348.
[21] S.E. Wellman, Y. Song, D. Su, N.M. Mamoon, Purification of mouse H1 histones expressed in *Escherichia coli*, Biotechnol. Appl. Biochem. 26 (Pt 2) (1997) 117–123.
[22] N.M. Mamoon, Y. Song, S.E. Wellman, Histone h1(0) and its carboxyl-terminal domain bind in the major groove of DNA, Biochemistry 41 (2002) 9222–9228.
[23] R.D. Wells, J.E. Larson, R.C. Grant, B.E. Shortle, C.R. Cantor, Physicochemical studies on polydeoxyribonucleotides containing defined repeating nucleotide sequences, J. Mol. Biol. 54 (1970) 465–497.
[24] H.K. Schlitz, Protein purification: Principles and practice, by R Scopes. Pp 282. Springer-Verlag, Berlin, Heidelberg and New York, 1982. DM 79. ISBN 3–540–90726–2 Biochem. Educ. 12 (1984) 143.
[25] V.H. Le, R. Buscaglia, J.B. Chaires, E.A. Lewis, Modeling complex equilibria in isothermal titration calorimetry experiments: thermodynamic parameters estimation for a three-binding-site model, Anal. Biochem. 434 (2013) 233–241.
[26] A. Velazquez-Campoy, Ligand binding to one-dimensional lattice-like macromolecules: analysis of the McGhee–von Hippel theory implemented in isothermal titration calorimetry, Anal. Biochem. 348 (2006) 94–104.
[27] D.M. Gray, A.R. Morgan, R.L. Ratliff, A comparison of the circular dichroism spectra of synthetic DNA sequences of the homopurine. Homopyrimidine and mixed purine–pyrimidine types, Nucleic Acids Res. 5 (1978) 3679–3695.
[28] S.Z. Hirschman, G. Felsenfeld, Determination of DNA composition and concentration by spectral analysis, J. Mol. Biol. 16 (1966) 347–358.
[29] W.C. Johnson Jr., Protein secondary structure and circular dichroism: a practical guide, Proteins 7 (1990) 205–214.
[30] J.L. Barbero, L. Franco, F. Montero, F. Moran, Structural studies on histones H1. Circular dichroism and difference spectroscopy of the histones H1 and their trypsin-resistant cores from calf thymus and from the fruit fly *Ceratitis capitata*, Biochemistry 19 (1980) 4080–4087.
[31] G.J. Carter, K. van Holde, Self-association of linker histone H5 and of its globular domain: evidence for specific self-contacts, Biochemistry 37 (1998) 12477–12488.
[32] N.K. Modukuru, K.J. Snow, B.S. Perrin Jr., A. Bhambhani, M. Duff, C.V. Kumar, Tuning the DNA binding modes of an anthracene derivative with salt, J. Photochem. Photobiol. A Chem. 177 (2006) 43–54.
[33] W.B. Tan, W. Cheng, A. Webber, A. Bhambhani, M.R. Duff, C.V. Kumar, G.L. McLendon, Endonuclease-like activity of heme proteins, J. Biol. Inorg. Chem. 10 (2005) 790–799.
[34] J. Allan, P.G. Hartman, C. Crane-Robinson, F.X. Aviles, The structure of histone H1 and its location in chromatin, Nature 288 (1980) 675–679.
[35] J.A. Subirana, Analysis of the charge distribution in the C-terminal region of histone H1 as related to its interaction with DNA, Biopolymers 29 (1990) 1351–1357.
[36] J. Allan, T. Mitchell, N. Harborne, L. Bohm, C. Crane-Robinson, Roles of H1 domains in determining higher order chromatin structure and H1 location, J. Mol. Biol. 187 (1986) 591–601.
[37] J. Bednar, R.A. Horowitz, S.A. Grigoryev, L.M. Carruthers, J.C. Hansen, A.J. Koster, C.L. Woodcock, Nucleosomes, linker DNA, and linker histone form a unique structural motif that directs the higher-order folding and compaction of chromatin, Proc. Natl. Acad. Sci. 95 (1998) 14173–14178.
[38] J. Zlatanova, C. Seebart, M. Tomschik, The linker-protein network: control of nucleosomal DNA accessibility, Trends Biochem. Sci. 33 (2008) 247–253.